

## Climbing Nitrogenase: Toward a Mechanism of Enzymatic Nitrogen Fixation

BRIAN M. HOFFMAN,<sup>\*,†</sup> DENNIS R. DEAN,<sup>‡,⊥</sup> AND  
LANCE C. SEEFELDT<sup>§,⊥</sup>

<sup>†</sup>Department of Chemistry, Northwestern University, 2145 Sheridan Road, Tech K148, Evanston, Illinois 60208, <sup>‡</sup>Department of Biochemistry, Virginia Polytechnic Institute and State University, 110 Fralin Hall, Blacksburg, Virginia 24061, <sup>§</sup>Department of Chemistry and Biochemistry, Utah State University, 0300 Old Main Hill, Logan, Utah 84322-0300

RECEIVED ON SEPTEMBER 26, 2008

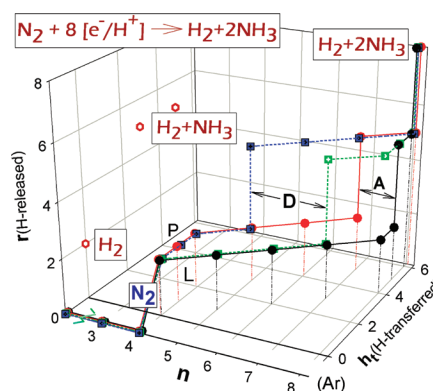
### CON SPECTUS

**N**itrogen fixation, the reduction of dinitrogen ( $N_2$ ) to two ammonia ( $NH_3$ ) molecules, by the Mo-dependent nitrogenase is essential for all life. Despite four decades of research, a daunting number of unanswered questions about the mechanism of nitrogenase activity make it the “Everest of enzymes”. This Account describes our efforts to climb one “face” of this mountain by meeting two interdependent challenges central to determining the mechanism of biological  $N_2$  reduction. The first challenge is to determine the reaction pathway: the composition and structure of each of the substrate-derived moieties bound to the catalytic FeMo cofactor (FeMo-co) of the molybdenum–iron (MoFe) protein of nitrogenase. To overcome this challenge, it is necessary to discriminate between the two classes of potential reaction pathways: (1) a “distal” (D) pathway, in which H atoms add sequentially at a *single* N or (2) an “alternating” (A) pathway, in which H atoms add alternately to the *two* N atoms of  $N_2$ . Second, it is necessary to characterize the dynamics of conversion among intermediates within the accepted Lowe–Thorneley kinetic scheme for  $N_2$  reduction. That goal requires an experimental determination of the number of electrons and protons delivered to the MoFe protein as well as their “inventory”, a partition into those residing on each of the reaction components and released as  $H_2$  or  $NH_3$ .

The principal obstacle to this “climb” has been the inability to generate  $N_2$  reduction intermediates for characterization. A combination of genetic, biochemical, and spectroscopic approaches recently overcame this obstacle. These experiments identified one of the four-iron Fe–S faces of the active-site FeMo-co as the specific site of reactivity, indicated that the side chain of residue  $\alpha 70V$  controls access to this face, and supported the involvement of the side chain of residue  $\alpha 195H$  in proton delivery. We can now freeze-quench trap  $N_2$  reduction pathway intermediates and use electron–nuclear double resonance (ENDOR) and electron spin–echo envelope modulation (ESEEM) spectroscopies to characterize them.

However, even successful trapping of a  $N_2$  reduction intermediate occurs without synchronous electron delivery to the MoFe protein. As a result, the number of electrons and protons,  $n$ , delivered to MoFe during its formation is unknown. To determine  $n$  and the electron inventory, we initially employed ENDOR spectroscopy to analyze the substrate moiety bound to the FeMo-co and  $^{57}Fe$  within the cofactor. Difficulties in using that approach led us to devise a robust kinetic protocol for determining  $n$  of a trapped intermediate.

This Account describes strategies that we have formulated to bring this “face” of the nitrogenase mechanism into view and afford approaches to its climb. Although the summit remains distant, we look forward to continued progress in the ascent.



## Introduction

“Nitrogen fixation”, the reduction of dinitrogen ( $N_2$ ) to two ammonia ( $NH_3$ ) molecules, is essential to all life, because it is essential to the input of nitrogen from  $N_2$  into the global biogeochemical N-cycle. The majority of  $N_2$  fixation occurs biologically, by the action of the microbial enzyme nitrogenase. There are four known types of nitrogenase, primarily distinguished by the metal composition of their active-site metaloclusters.<sup>1</sup> The most important is the Mo-dependent enzyme<sup>2</sup> on which this Account focuses, hereafter denoted, “nitrogenase”. It comprises two components, denoted the MoFe and Fe proteins. The former contains the active-site, multimetallic iron–molybdenum cofactor (FeMo-co) cluster, as well as an auxiliary “P” cluster, presumed to mediate electron transfer from Fe protein to FeMo-co. The Fe protein contains a [4Fe–4S] cluster and delivers electrons one-at-a-time to the MoFe protein.

Nitrogenase has been subjected to four decades of intensive kinetic<sup>3,4</sup> and spectroscopic studies,<sup>2</sup> and structures have been determined for MoFe and Fe proteins and for multiple forms of their complex.<sup>5</sup> Given the remarkable insights these studies provide into nitrogenase structure and function, one might expect that we would be well on the way to understanding the full mechanism of biological  $N_2$  fixation. However, as outlined by Howard and Rees<sup>6</sup> and Schrock,<sup>7</sup> a daunting number of mechanistic questions remain unanswered, in our view making nitrogenase the “Everest of enzymes”. This Account describes our efforts to climb one “face” of this mountain by meeting two interdependent challenges that are central to determining the mechanism of biological  $N_2$  reduction. The first is to determine the reaction pathway for  $N_2$  reduction. The second challenge is to characterize the dynamics of conversion among intermediates by incorporating them into a “multidimensional” formulation of the accepted Lowe–Thorneley (LT) kinetic scheme for  $N_2$  reduction.<sup>2–4</sup> This task in turn requires an experimental determination for each intermediate of  $n$ , the number of electrons or protons delivered to MoFe protein, as well as the “electron or proton inventory route” for catalysis, a partition of each intermediate’s  $n$  electrons or protons into those residing on FeMo-co, those residing on the substrate-derived moiety bound to it, and those released as  $H_2$  or  $NH_3$ . These efforts seek some of the enzyme’s most closely held secrets. This Account both describes the barriers to ascent and summarizes recent progress<sup>8–10</sup> in experiment and concept that are slowly advancing us toward the summit.

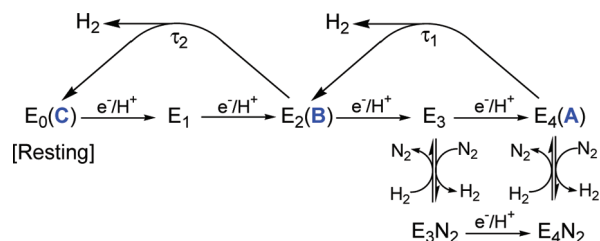
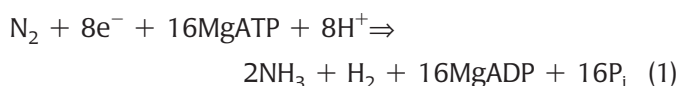


**FIGURE 1.** Early stages of Lowe–Thorneley (LT) kinetic scheme for  $N_2$  reduction, the portion that connects states  $E_0$  through  $E_4$ ; for a full scheme, see refs 2–4. As discussed in conjunction with Figure 8, **A** is the MoFe protein “hydride” intermediate; **B** forms during its relaxation to resting state, **C**.

## The First Decades

$NH_3$  formation by nitrogenase proceeds through a series of intermediates in which  $N_2$  and its reduced forms bind to FeMo-co.<sup>2,3</sup> However, during the first four decades of studying purified nitrogenase, no reduction intermediate was trapped for characterization, although intermediates that accumulate during CO inhibition were trapped early on.<sup>11,12</sup> Instead, the 1970s and 1980s witnessed the formulation of a kinetic scheme for substrate reduction, with some insights into the nature of intermediates being provided by studies of pre-steady-state kinetics. These efforts culminated in the LT kinetic scheme,<sup>2–4</sup> which has proven to satisfactorily describe the kinetics of nitrogenase catalysis in full.

Such efforts surprisingly showed that nitrogen fixation under optimized conditions exhibits the reaction stoichiometry



Thus, the enzymatic reaction is both expensive, requiring the hydrolysis of two MgATP per reducing equivalent, and curious, in that eight reducing equivalents, not six, are needed to reduce each  $N_2$  to two  $NH_3$ , with two equivalents being “wasted” through the evolution of  $H_2$ .<sup>2,3</sup>

The LT scheme, shown in part in Figure 1, is formulated in terms of states, denoted  $E_n$ , that are indexed by the number of electrons and protons,  $n$ , that have been delivered to the MoFe protein during their formation,  $n = 0$  (resting)  $\leftrightarrow 8$  (as required by eq 1); it is characterized by the rate constants for transformations among those states. Particular features of note include the following: during catalysis, the Fe protein delivers one electron at a time to the MoFe protein as its 4Fe–4S cluster cycles between (1+) and (2+) oxidation states; protein complex formation and single-electron transfer from Fe protein to MoFe protein is driven by the binding and hydrolysis of two MgATP within the Fe protein; the release of the Fe protein after delivery of its electron is the rate-limiting step of

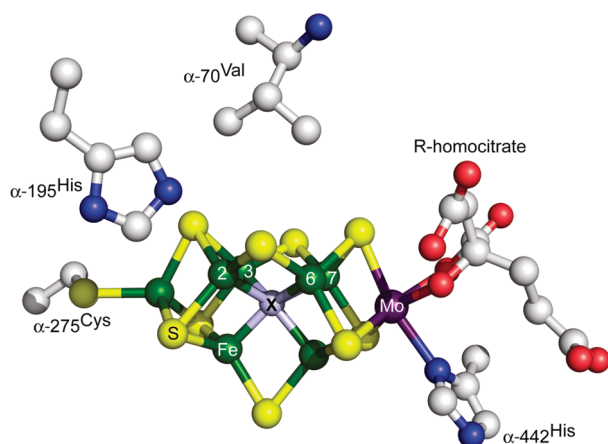


**FIGURE 2.** Structure of FeMo-co, including the two residues that covalently link it to the apoprotein and the two implicated in function,  $\alpha$ -V70 as substrate “gatekeeper” and  $\alpha$ -H195 as agent for proton delivery.

catalysis.<sup>3</sup>  $N_2$  reduction involves eight of these cycles to deliver the eight electrons necessary for substrate binding and reduction, eq 1.

There is little evidence for binding of any substrate to the resting state of the MoFe protein, and  $N_2$  does not appear to bind until the MoFe protein has been activated by the accumulation of three or four electrons and protons ( $E_3$  or  $E_4$ ).<sup>3</sup> In the absence of other substrates, activation of MoFe protein leads to the reduction of protons to form  $H_2$ , with the protein thereby cycling back to its resting state. In the presence of  $N_2$ , this hydrogenase capability leads to a competition between  $H^+$  and  $N_2$  reduction. As a result, even the optimum stoichiometry of one  $H_2$  formed per  $N_2$  reduced (eq 1) represents only a lower limit.

The X-ray structure of MoFe protein was first determined 16 years ago.<sup>5</sup> It revealed the active-site FeMo cofactor to be an unprecedented  $[Fe_7S_9Mo; \text{homocitrate}]$  cluster, Figure 2, with roughly trigonal symmetry along the terminal Fe–Mo axis. Subsequently, refinement showed the presence in FeMo-co of an interstitial first-row atom,  $X = C, N, \text{ or } O$ , making its final composition,  $[Fe_7S_9MoX; \text{homocitrate}]$ ,<sup>13</sup> and structures were obtained for multiple  $[Fe; \text{ MoFe}]$  protein complexes.<sup>5</sup>

The structure of FeMo-co (Figure 2) was a major surprise, and its determination provides the foundation for any discussion of mechanism. But in some ways, it deepened the mystery. First, examination of the resting-state structure does not reveal the site of  $N_2$  binding and reduction! Mo is an obvious candidate for the active site, because it is incorporated in the only known inorganic metal complexes that catalytically reduce  $N_2$ .<sup>14</sup> However, Fe is an equally attractive candidate, given that it is the catalytic metal in the commercial

Haber–Bosch process for  $NH_3$  formation and that there are V and Fe nitrogenases that reduce  $N_2$  but do not have Mo.<sup>15</sup> Then, if Fe is involved, the structure does not indicate which of the three  $4Fe-4S$  “faces” of the central  $[Fe_6]$  iron prismane is active, much less identify the active Fe(s). In addition, there are such questions as why homocitrate<sup>16</sup> and what is X?<sup>17</sup>

Thus, at the beginning of this millennium we knew the structure of nitrogenase in its resting state but not where catalysis occurred within that structure. Kinetics measurements culminating in the LT scheme provided an excellent understanding of how nitrogenase converts among the  $E_n$  intermediates during  $N_2$  reduction, but we had absolutely no experimental evidence as to the identity and structure of any of these intermediates.

## What Is the Problem?

The LT scheme reveals that the major obstacle to generating an  $E_n$  intermediate in sufficient amounts for characterization and thus perhaps the reason for such an unsatisfying state of affairs is that the MoFe protein acquires electrons one-at-a-time from its partner Fe protein and this process involves the nucleotide-dependent *association and dissociation* of the two proteins.<sup>2</sup> As a consequence, multiple electron additions to MoFe protein cannot be synchronized, for complex *dissociation* represents the rate-limiting step of substrate reduction,<sup>2,3</sup> while electron accumulation is opposed by the competing loss of  $H_2$ . EPR has been the primary tool in monitoring nitrogenase under turnover, and efforts to trap turnover intermediates for study indeed showed loss of the resting-state FeMo-co EPR signal under turnover, indicating that it has converted to intermediate  $E_n$  states. However, no signals from such states appeared in its place, indicating that the system distributes itself among multiple intermediates or that the preponderant states are EPR-silent or both. This barrier to study contrasts, for example, with the ready use of flash photolysis in photosynthesis to synchronously generate a particular desired intermediate for study.<sup>18</sup>

## Beginning an Ascent

A way up this face was revealed<sup>9,10</sup> in a series of studies that combined genetic, biochemical, and spectroscopic approaches that (i) identified the specific site of reactivity as the  $4Fe-4S$  face of FeMo cofactor defined by Fe atoms 2, 3, 6, and 7 (numbering based on pdb 1M1N), (ii) demonstrated that the side chain of residue  $\alpha$ 70V acts as a “gatekeeper” that controls access to the FeMo-co active site, and (iii) supported the

idea that proton delivery involves the side chain of residue  $\alpha 195\text{H}$ .<sup>10,19,20</sup> These structural features all are shown in Figure 2.

These conclusions stem from the observation that decreasing the size of the  $\alpha 70\text{V}$  residue by substitution with alanine allows the enzymatic reduction of molecules excluded from the wild-type (WT) active site, such as propyne, propargyl alcohol, and 1-butyne, while increasing its size by substitution with isoleucine represses reaction of all WT substrates except  $\text{H}^+$ .<sup>9,10</sup> In both variants, the change leaves the reactivity of FeMo-co unaltered. These observations were accompanied by the discovery that reduction intermediates could be trapped in MoFe variants with mutations at  $\alpha 70\text{V}$ ,  $\alpha 195\text{H}$ , or both and subsequently in WT enzyme itself.<sup>10</sup> This discovery opens a trail to the summit.

## Intermediates

Beginning in 2004, a series of reports described the first freeze–quench trapping and characterization of enzymatic intermediates,<sup>8,9</sup> initially ones that form during the reduction of alkyne substrates,<sup>21,22</sup> then one formed during the reduction of  $\text{H}^+$  under Ar,<sup>23</sup> then four intermediates associated with  $\text{N}_2$  reduction.<sup>24–27</sup> In all but one of these cases, a key was the use of MoFe proteins that contain the amino acid substitutions, separately or in combination, that inhibit proton delivery to substrates ( $\alpha 195^{\text{Gln}}$ ) and modulate substrate accessibility to the reduction site ( $\alpha 70^{\text{Ala}}$ ). The trapping of an intermediate during  $\text{N}_2$  reduction by WT nitrogenase supports the view that these intermediates reflect normal nitrogenase function. They are being characterized biochemically, and as is now illustrated, their structures are being determined by the spectroscopic methods of choice, electron nuclear double resonance (ENDOR) and electron spin–echo envelope modulation (ESEEM).<sup>28,29</sup>

**CO, Alkyne, and Hydride.** The first use of ENDOR to study any nitrogenase intermediate employed  $^{57}\text{Fe}$  to prove that the EPR signals from the two CO-inhibited forms of the MoFe protein arise from the FeMo cofactor, not the P cluster,<sup>30</sup> used  $^{13}\text{C}$  ENDOR to demonstrate that one CO binds to the “lo-CO” state formed under low CO pressure while two bind to “hi-CO”, and offered proposals for the CO binding modes.<sup>31</sup>

The first determination of the structure of a nitrogenase catalytic intermediate combined  $^{13}\text{C}$  and  $^1\text{H}$  Mims 35 GHz ENDOR techniques to reveal the structure of the substrate-derived moiety bound to FeMo-co in the intermediate formed during reduction of the alkynes propargyl alcohol (PA;  $\text{HC}\equiv\text{CHCH}_2\text{OH}$ )<sup>21</sup> and  $\text{HC}\equiv\text{CH}$ <sup>22</sup> by MoFe variants. This study provides the “template” for the ongoing applications of

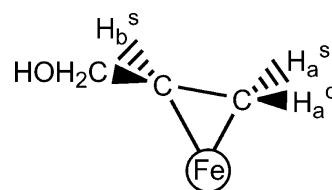
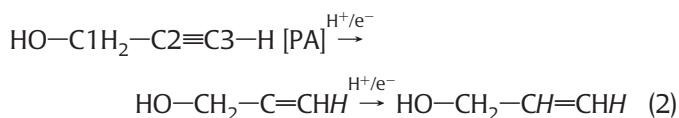


**FIGURE 3.** Proposed structure for the intermediate trapped during propargyl alcohol reduction, the product alkene bound side-on to a single Fe ion.

ENDOR/ESEEM spectroscopies to determine structure in such a complicated system. These techniques in general do not provide sufficient information with which to directly deduce the nature and binding geometry of the substrate-derived moiety, and quantum mechanical computations on FeMo-co are not advanced enough to unambiguously interpret the hyperfine/quadrupole couplings that are measured. Instead, the measurements supply constraints against which possible models can be tested and the correct model selected.

In the case of the PA intermediate,<sup>21</sup>  $^{13}\text{C}$  ENDOR showed that the PA backbone remains intact and is covalently bonded to FeMo-co and that no two of the backbone  $^{13}\text{C}$ 's are equivalent. Thus, there are only three possible species that might be bound to FeMo-co: PA itself, singly reduced PA, or the alkene product (allyl alcohol), eq 2.



$^1\text{H}$  ENDOR further disclosed that the terminal carbon (C3) of PA carries a nonexchangeable H of the reactant and a solvent-derived H and that the two are symmetry-equivalent through a reflection in a  $g$ -tensor plane. In addition, there is another, more weakly coupled, solvent-derived H, indicated in italic. Upon testing these constraints against every relevant structure in the Cambridge Structural Database, we reached the remarkable conclusion that the intermediate contains a bioorganometallic complex, the alkene reduction product, allyl alcohol, bound “side-on” to one Fe of FeMo-co (Figure 3), and a similar conclusion was shown to apply to the corresponding intermediate trapped during  $\text{C}_2\text{H}_2$  reduction.<sup>22</sup> Subsequent experiments and DFT computations supported this conclusion.<sup>9</sup>

PA is not a substrate of WT nitrogenase but becomes one when substrate access is expanded by reducing the size of the  $\alpha\text{-V70}$  side chain through the  $\alpha\text{-V70A}$  amino acid substitution. If the size of this side chain is instead increased through the  $\alpha\text{-V70I}$  substitution, the result is a MoFe protein variant effective only in the reduction of  $2\text{H}^+$  to  $\text{H}_2$ . During turnover under Ar, this variant accumulates a novel intermediate that

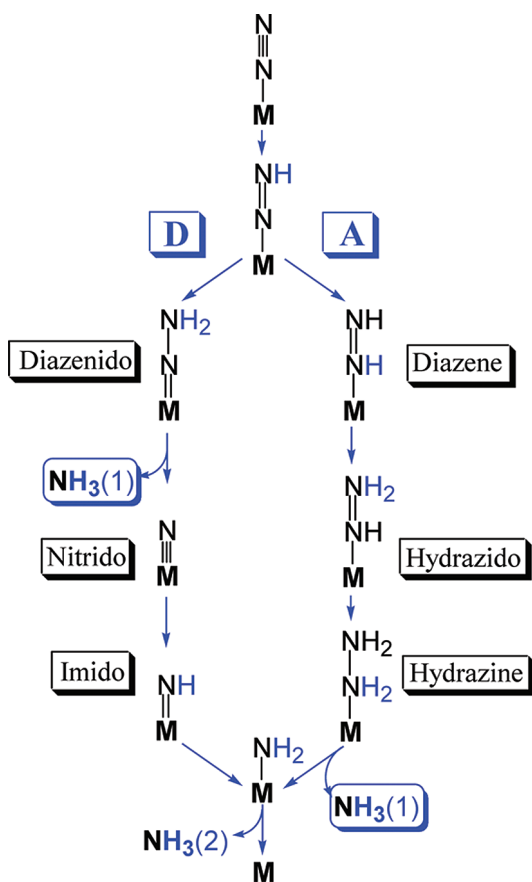


**FIGURE 4.** “Alternating” (A) and “distal” (D)  $N_2$  reduction pathways. M represents FeMo-co without specifying metal ion(s) involved. Likewise, the representations of binding are meant to emphasize the distinction between pathways and do not imply specific binding modes. Small straight arrows represent addition of  $H^+/e^-$  to substrate.

was shown by  $^1H$  ENDOR to have two chemically equivalent hydrides bound to metal ions of FeMo-co;<sup>23</sup> the central role of this intermediate in  $N_2$  reduction is discussed below.

**$N_2$  Intermediates and the Reaction Pathway.** A molecular mechanism of  $N_2$  reduction must include three constituents: (i) the “reaction pathway”, an enumeration of the states that arise during the conversion of reactants to products, (ii) the molecular structures of these intermediates, and (iii) a kinetic scheme, in this case the LT scheme, that incorporates information about the kinetics/dynamics of conversion among these intermediates. Considering constituent i, we recently formalized the division of  $N_2$  reduction pathways into two classes. In a “distal” (D) pathway, H-atoms add sequentially to a *single* N prior to N–N bond cleavage after the third hydrogenation, Figure 4. Catalytic  $NH_3$  formation at mononuclear Mo metal complexes follows such a pathway, as shown by the early work of Chatt and co-workers<sup>32</sup> and recently by Schrock and co-workers.<sup>14</sup> This contrasts with an “alternating” (A) pathway in which H-atoms add alternately to the *two* N atoms of

$N_2$  before N–N bond cleavage at the fifth hydrogenation, Figure 4, often favored in computational studies, for example.<sup>33</sup> Interestingly, current discussions of possible reduction mechanisms have tended to support one or the other class without explicitly noting that there are two classes, although this was well understood in early days.<sup>34</sup>

Until recently, the limited information about the nitrogenase pathway was predominately derived from kinetics studies, and these were interpreted as supporting the D version.<sup>3</sup> Because the substrate-derived species bound to FeMo-co along the alternative pathways of  $N_2$  reduction are different at many stages of  $N_2$  fixation, Figure 4, the enzyme’s pathway would be revealed if these species could be characterized by ENDOR/ESEEM. Thus it was of pivotal importance when in 2004 we first reported the successful trapping of intermediates associated with  $N_2$  reduction.<sup>25</sup> To date, four such  $S = 1/2$  states have been trapped:<sup>9,10,24–27</sup>  $e(N_2)$ , an early stage in reduction obtained from wild-type MoFe protein with  $N_2$  as substrate;<sup>25</sup>  $m(NH=N-CH_3)$ , from  $\alpha 195Gln$  MoFe protein with  $CH_3-N=NH$  as substrate;<sup>25,26</sup>  $m(N_2H_2)$  prepared<sup>27</sup> by freeze-quenching the MoFe protein  $\alpha 70Ala/\alpha 195Gln$  variant during steady-state turnover with *in situ* generated diazene;  $l(N_2H_4)$ , from  $\alpha 70Ala/\alpha 195Gln$  MoFe protein with  $H_2N-NH_2$  as substrate.<sup>24,25</sup>

A combination of  $^{15}N$  and  $^1H$  ENDOR measurements (Figure 5) showed that three of the intermediates  $l(N_2H_4)$ ,  $m(N_2H_2)$ , and  $m(NH=N-CH_3)$  contain a substrate-derived  $[-NH_x]$  moiety bound to the cofactor.<sup>24–27</sup> In contrast, FeMo-co of  $e(N_2)$  appears to bind a nonprotonated N, which would indicate that  $e(N_2)$  represents an earlier step in the catalytic pathway.<sup>25</sup> Recent  $^{14,15}N$  and  $^1H$  ENDOR measurements showed that the substrate-derived moiety in turnover states trapped with diazene and hydrazine substrates have extremely similar characteristics.<sup>27</sup> Hydrazine is well-known to be a *bona fide* nitrogenase substrate,<sup>35</sup> and biochemical experiments showed that the same holds for diazene.<sup>27</sup> Together, the above observations indicate that diazene enters the normal  $N_2$  reduction reaction pathway (Figure 4) and further suggest that during turnover and freeze–quench, diazene is reduced by the enzyme until it “catches up” to the species trapped during turnover with hydrazine, with the two substrates thus generating a common intermediate that falls along the normal pathway of  $N_2$  reduction by nitrogenase. If this speculation proves to be correct, considerations of Figure 4 show that it would favor an A mechanism.

Full characterization of these possibly common intermediates and of the others by ENDOR and by relaxation methods discussed below would definitively test this suggestion. How-

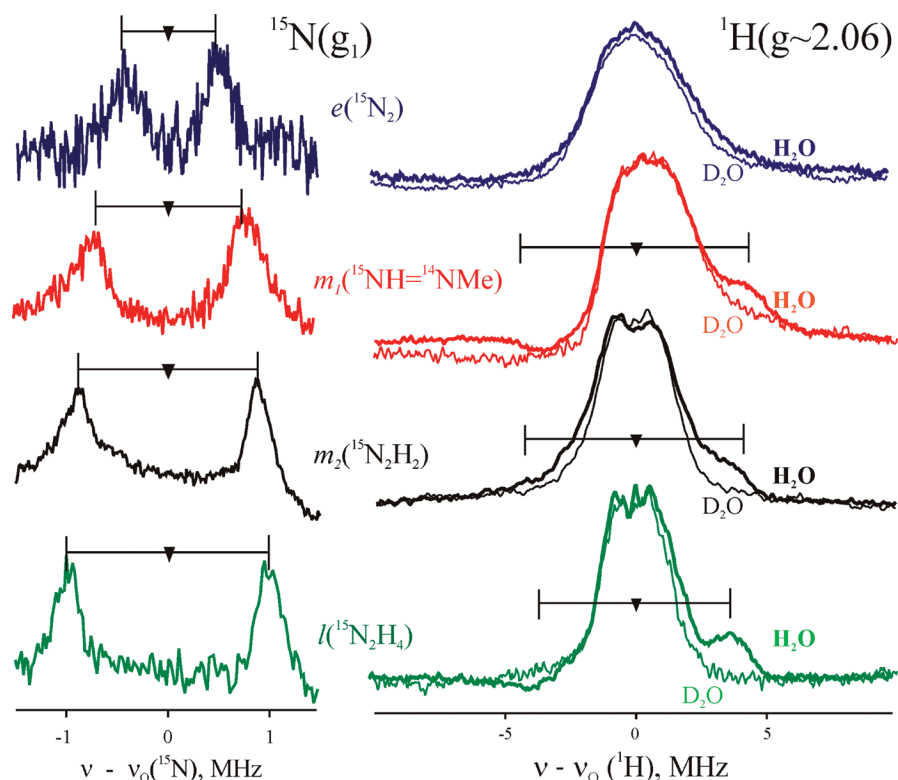
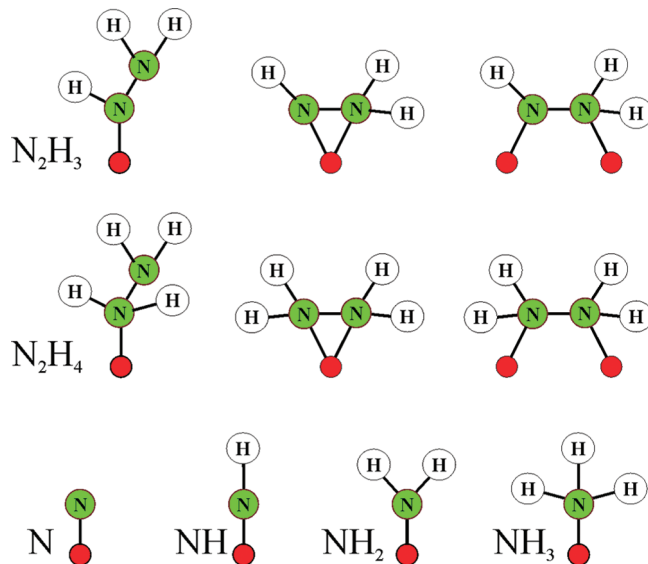


**FIGURE 5.** (left) Q-band Mims (e and m) and Re-Mims (l)  $^{15}\text{N}$ -ENDOR spectra ( $g_1$ ) of nitrogenous trapped intermediates labeled with  $^{15}\text{N}$  as indicated. Conditions: microwave frequency = 34.808–34.819 GHz;  $\pi/2 = 52$  ns (e, m) and 32 ns (l); RF = 20–30  $\mu\text{s}$ ;  $\tau = 500$  ns (e), 300 ns (m), and 200 ns (l); sampling =  $\sim 1000$  transients/point; repetition rate = 100 Hz (e and m) and 50 Hz (l); 2 K. (Right) CW  $^1\text{H}$ -ENDOR of  $^{14}\text{N}$  intermediates in  $\text{H}_2\text{O}$  and  $\text{D}_2\text{O}$ . Conditions: microwave frequency, 35.057–35.171 GHz; modulation amplitude = 4 G; RF sweep speed = 1 MHz/s; bandwidth of RF broadened to 100 kHz; 2 K.

ever, the use of  $^1\text{H}$  and  $^{14,15}\text{N}$  ENDOR/ESEEM to determine the structures of the trapped nitrogenous reduction intermediates is a much more formidable task than was the determination of the structure of the alkyne reduction intermediates. First, there are six stages of  $\text{N}_2$  reduction, not two (eq 1). Second, when alternate A/D pathways are taken into account (Figure 4), there are numerous possible  $[\text{N}_x\text{H}_y]$  species to be considered at every stage of  $\text{N}_2$  reduction; this is illustrated by Chart 1 for later stages. Third, one has less control over the placement of nuclear-spin probes. Because the  $\text{N}_2\text{H}_m$  ( $m = 0, 2, 4$ ) substrates used to generate intermediates are symmetric, unlike PA, selective labeling of the N's thus is impossible, except with the unnatural substrate  $\text{NH}=\text{N}-\text{CH}_3$ ;<sup>26</sup> all the N–H are solvent exchangeable, so selective deuteration as with PA also is impossible. On the other hand, just a very few ENDOR-derived constraints can act as powerful means of narrowing the list of candidates. To characterize a  $[\text{N}_y\text{H}_x]$  cofactor-bound moiety, one must answer the following questions: (i) is the N–N bond broken ( $y = 1$  or 2), and if not, are the two N's equivalent; (ii) what is the reduction level of the bound fragment (what is  $x$ ); (iii) what is the binding mode if  $y = 2$ ? Some of these constraints will come directly from ENDOR results for

**CHART 1.** Substrate-Derived Species Bound to FeMo-co That Might Form in Late Stages of  $\text{N}_2$  Reduction



the intermediates, as complemented and strengthened by comparisons<sup>36</sup> with newly emerging biomimetic complexes,<sup>37,38</sup> but some will come from a relaxation-kinetics protocol to be described below.

## Connecting Intermediates and Kinetics<sup>22,39</sup>

The nitrogenase reaction pathway is specified by determination of the composition and structure of the intermediates of N<sub>2</sub> reduction, Figure 4. However, even when a N<sub>2</sub> reduction intermediate has been trapped, this occurs without synchronous electron delivery to the MoFe protein. As a result, the number of electrons and protons,  $n$ , delivered to MoFe during its formation is unknown, and the intermediate is untethered from the LT kinetic scheme for substrate reduction. Thus,  $n$  for the intermediate must be determined, but beyond this, one must determine how those electrons and protons are partitioned: are they on FeMo-co, P cluster, or substrate? One may loosely define an “N<sub>2</sub> reduction mechanism” as comprising complete answers to three conjoined questions for all intermediates: composition and structure, the value of  $n$ , and the partition of  $n$ . The next section discusses efforts to address the second and third of these.

**Electron Inventory.** The first effort to determine  $n$  for an intermediate focused on those generated during alkyne reduction. It introduced the concept of a MoFe protein “electron inventory”,<sup>22</sup> seeking to determine the number ( $n$ ) of electrons and protons that have been delivered to the MoFe protein to form an E <sub>$n$</sub>  state by partitioning  $n$  into distinct categories and determining the number in each: those that reside on the substrate-derived moiety bound to FeMo-co ( $s$ ); those that remain on FeMo-co ( $m$ ); the number of electrons and protons that have been “released” ( $r$ ) through liberation of H<sub>2</sub> and reduced substrate (e.g., NH<sub>3</sub>); further allowing for the possibility that P cluster has donated ( $p$ ) electrons to FeMo-co. The index,  $n$ , thus can be written as the sum over categories:<sup>22</sup>

$$n = m + s + r - p \quad (3)$$

For the alkyne intermediates,  $r = p = 0$ , so  $n = m + s$ . The idea was to use ENDOR of nuclei associated with the substrate-derived moiety bound to FeMo-co to determine  $s$  and <sup>57</sup>Fe ENDOR of FeMo-co to determine  $m$ .

The inventory concept implicitly recognizes that the single index,  $n$ , is inadequate to specify the properties of an intermediate and that additional indices are needed. For example, as in other formal valency schemes, the inventory depends on the nature of the binding of substrate-derived fragments to FeMo-co. Consider the E <sub>$n$</sub>  intermediate that contains the ethylene product of acetylene reduction bound to FeMo-co. If ethylene acts as a dative  $\pi$ -donor ( $\pi$ -C<sub>2</sub>H<sub>4</sub>; Figure 6), this binding does not alter the formal reduction level of the FeMo-co ( $m$ ) or the alkene ( $s = 2$ ), and the complex has an electron inventory,  $n = m + s = m + 2$ . However, one might instead imag-

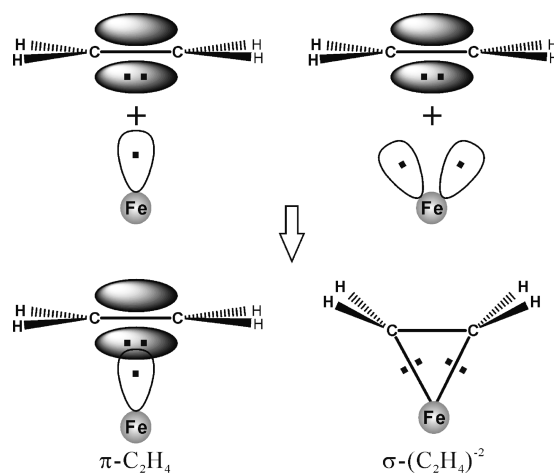


**FIGURE 6.** Cartoon representation of alternate schemes for binding C<sub>2</sub>H<sub>4</sub> to a cofactor metal ion: (left) dative  $\pi$  bonding; (right) oxidative addition to form Fe–C  $\sigma$  bonds.

ine that C<sub>2</sub>H<sub>4</sub> actually binds through C–Fe  $\sigma$ -bonds as the ferracyclopropane ( $\Phi$ -C<sub>2</sub>H<sub>4</sub>; Figure 6). Such a structure corresponds to oxidative addition of C<sub>2</sub>H<sub>4</sub> to the FeMo-co, and in this case the alkene must be described formally as having accepted two additional electrons from FeMo-co, making a total of  $s = 4$  electrons transferred to the initial C<sub>2</sub>H<sub>2</sub> substrate. As a result,  $n = m + 4$ . Analysis of <sup>57</sup>Fe ENDOR measurements of the acetylene-reduction intermediate, in combination with a variety of other considerations, led us to prefer  $n = 4$  for this intermediate, compatible with the finding of Lowe et al. that C<sub>2</sub>H<sub>4</sub> is released from the E<sub>3</sub> and E<sub>4</sub> states during C<sub>2</sub>H<sub>2</sub> reduction by WT enzyme.<sup>40</sup> Thus, depending upon the binding mode, the E<sub>4</sub> MoFe protein would have accumulated four electrons, but FeMo-co of this intermediate could formally retain  $m = 2$  electrons ( $\pi$ -C<sub>2</sub>H<sub>4</sub>; Figure 6) or none,  $m = 0$  ( $\Phi$ -C<sub>2</sub>H<sub>4</sub>). This proposed  $n$  will be tested with a kinetic procedure described below.

**Inventory Routes and the LT Scheme in 3D.** Once one introduces the concepts of electron and proton inventories for intermediates, it becomes clear that there are not just two alternative pathways for the sequential addition of electrons and protons to substrate, D and A (Figure 4), but each represents a multiplicity. For example, according to the LT scheme (Figure 1), N<sub>2</sub> binding to the E<sub>4</sub> state of nitrogenase occurs with loss of two electrons and protons as H<sub>2</sub>, leaving N<sub>2</sub>-bound FeMo-co reductively activated by the remaining  $m = 2$  electrons. But these electrons can in principle be delivered to substrate at any subsequent stage in the reaction, and thus the A and D pathways in Figure 4 each really represents many possible “electron inventory routes” of reduction. As one limiting route, transfer of the  $m = 2$  electrons and protons to N<sub>2</sub> could occur promptly (P) to form bound diazene; in the opposite

limit, these electrons might remain on FeMo-co until the final, late (L), stages of  $N_2$  reduction; and of course there are intermediate cases. To describe the alternative intermediate states embodied in these multiple pathways/routes requires other “quantum numbers” in addition to  $n$ . In this light, the LT scheme as typically drawn (e.g., Figure 1) is best viewed as a 1D projection of a “multidimensional” kinetic scheme.

One way to represent such a scheme is to extend the notation for an  $E_n$  intermediate formed during  $N_2$  reduction so as to include indices that specify the electron ( $e$ ) inventory (eq 3):  $E_n[m,s,r,p]^e$ . However, as indicated above, an *electron* inventory in general is as much a formal construct, analogous to formal atomic valencies in a molecule, as an experimental one. Instead, it seems more instructive to denote an  $E_n$  intermediate by its “proton (H) inventory”. Because each electron delivered to MoFe protein is accompanied by a proton,  $n = n(e^-) = n(H^+)$ , we may denote the multiple possible intermediates at the  $E_n$  stage of reduction by specifying  $h_m$ , the number of protons that remain bound to cofactor as protonated sulfide or hydride,  $h_s$ , the number that are associated with the substrate-derived moiety bound to FeMo-co, and  $r$ , the number of protons and electrons that have been released as  $H_2$  or reduced substrate or fragment. The proton inventory analogue to eq 3 then equates the sum of these protons to  $n$ :

$$\begin{aligned} n &= h_m + h_s + r \\ &\equiv h_m + h_t \end{aligned} \quad (4)$$

where we further define the total number of protons that have been transferred to substrate, regardless of their fate:  $h_t = [h_s + r]$ . For clarity, we will sometimes denote an intermediate as,  $E_n[h_m, h_s, r]^H$ , but in fact, for a given  $n$  the alternate intermediates can be specified with only two “quantum numbers”:  $[h_m, h_s]$ ,  $[h_m, r]$ , or  $[h_t, r]$ ; the remaining index is fixed by eq 4. For completeness, one should further incorporate into the notation the substrate-derived species ( $S$ ) bound to FeMo-co, leading to a notation in which the alternate intermediates associated with a given value of  $n$  may be written in terms of the three inventory indices,  $E_n[h_m, h_s, r; S]^H$ , or more economically in terms of two, as  $E_n[h_t, r; S]^H$ , etc. An advantage of this approach is that it is not merely formal: a proton on FeMo-co is a “classical” particle; it really is bound either to an atom of substrate or to one of FeMo-co.

Figure 7 presents a 3D proton inventory plot that displays the four *limiting* alternate routes of  $N_2$  reduction that involve  $N_2$  binding to  $E_4$  with release of  $H_2$ : D vs A pathways, each with either prompt (P) or late (L) transfer to substrate of the  $m = 2$  electrons and protons that remained on MoFe after  $N_2$  binding. The plot omits the corresponding routes associated

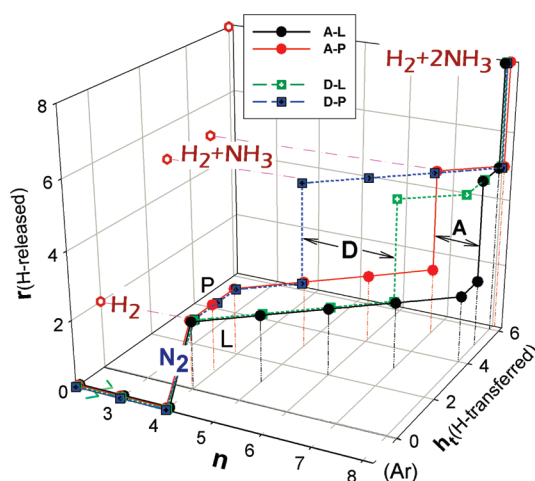


**FIGURE 7.** 3D representation of LT scheme plotted in terms of the proton inventory (eq 4), showing the alternative limiting reaction pathways for  $N_2$  reduction by nitrogenase that begin with  $N_2$  binding to intermediate  $E_4$  of Figure 1; formation of  $E_4$  is shown as occurring along its own “line” of electron accumulation. Indices of intermediate states are  $n$  (abscissa);  $h_s$  (ordinate) = number of protons delivered to substrate;  $r$  (z axis) = number of electrons and protons released during catalysis. Pathways: alternating-late, A-L (black); alternating-prompt, A-P (red); distal-late, D-L (green); distal-prompt, D-P (blue).

with  $N_2$  binding at  $E_3$  because their inclusion would make it unreadable. In this plot, the alternate proton inventories available for  $E_n$  are denoted  $E_n[h_t, r; S]^H$ , with a particular inventory route represented by a series of points for which the abscissa is  $n$ , the ordinate is  $h_t$ , and the z coordinate is  $r$ , the number of protons (and electrons) released as  $H_2$  and  $NH_3$  during catalysis.

The routes displayed begin with the accumulation of  $n = 4$  electrons and protons to generate the “hydride” intermediate activated for  $N_2$  binding,  $E_4[h_t=0, r=0]^H$ , and hence  $m = 4$  from eq 4. Next,  $N_2$  binding and the accompanying release of  $H_2$  ( $r = 2$ ) generates  $E_4[0, 2]^H$ , with  $m = 2$ . The P and L routes then diverge, each subsequently splitting into D and A branches. Release of the first  $NH_3$  ( $r = 5$ ) occurs at a different state on each of the four branches; the four finally converge to release the second  $NH_3$  ( $r = 8$ ). The volume enclosed by these limiting paths contains the points for states that would arise in a “mixed” pathway.

This approach also helps in thinking about such enduring mysteries as why is release of  $H_2$  an obligatory feature of  $N_2$  binding (eq 1), why must  $N_2$  bind to MoFe protein that has acquired  $n = 4$  electrons and protons (Figure 4), written most descriptively with the three inventory indices as state  $E_4[h_m, h_s, r; -]^H = E_4[4, 0, 0; -]^H$ , when the accompanying loss of  $H_2$  yields an  $N_2$ -bound state in which MoFe protein retains only two equivalents,  $E_4[2, 0, 2; N_2]^H$ , and analogously for bind-

ing to  $n = 3$ ? Consider the “overpotential” requirement, that  $N_2$  bind to a state with  $n > 2$ . If it were to be shown that catalysis follows a P route in which, for example,  $E_4[4,0,0;-]^H$  binds  $N_2$  and loses  $H_2$  to form  $E_4[2,0,2;N_2]^H$ , with prompt followup reduction of  $N_2$  to generate  $E_4[0,2,2;N_2H_2]^H$ , then one could interpret this overpotential as reflecting a need to reductively stabilize bound  $N_2$ . On the other hand, if an L route is operative, for example, with the  $e(N_2)$  intermediate corresponding to  $E_4[2,0,2;N_2]^H$ , then one might speculate that the required high level of reduction ( $n = 4$  or  $3$ ) is accompanied by a structural rearrangement of the FeMo cofactor that is required for  $N_2$  binding.

**Relaxation Protocol.** The use of an “electron inventory” to determine  $n$  for intermediates other than those trapped during alkyne reduction was blocked by several difficulties, one being that the effects of slow  $^{57}\text{Fe}$  nuclear relaxation made it difficult to analyze  $^{57}\text{Fe}$  ENDOR spectra. This led us to devise a robust new kinetic protocol for determining the  $E_n$  state of a trapped intermediate.<sup>39</sup> It is founded on the recognition that no matter how an intermediate state of the MoFe protein has been trapped, it has accumulated a specific number of electrons,  $n$ , and it is in a specific  $E_n$  state. Thus, it acts as a “synchronously prepared” initial state. In particular, we hypothesized that  $n$  for an intermediate state early in the kinetic scheme (Figure 1) could be revealed by following its “synchronous” relaxation back to the resting state ( $E_0$ ) through the loss of one or more equivalents of  $H_2$  and “simply” counting the number of such  $\Delta n = -2$  steps.

This approach, of course, requires that no additional electrons transfer from Fe protein to MoFe protein during the relaxation, which raises the question: How can one “turn off” intercomponent electron transfer without perturbing the MoFe protein in a sample that retains both the reducing equivalents and ATP required for this electron transfer? The answer rests in the fact that each ET from the Fe protein to the MoFe protein absolutely requires dissociation and association of the Fe–MoFe protein complex.<sup>2,3</sup> We recognized that this electron transfer would be abolished if Fe–MoFe association and dissociation were prevented by keeping the sample frozen, while we knew from our studies of heme monooxygenases<sup>41</sup> that reactions within the MoFe protein can proceed in the frozen state. In the resulting relaxation protocol, a 77 K freeze-trapped intermediate relaxes in the solid (typically at 253 K) without additional intercomponent electron transfer, while reaction progress is monitored periodically by cooling the sample to 2 K for EPR measurements of the EPR-active species, at which temperature no reactions occur.

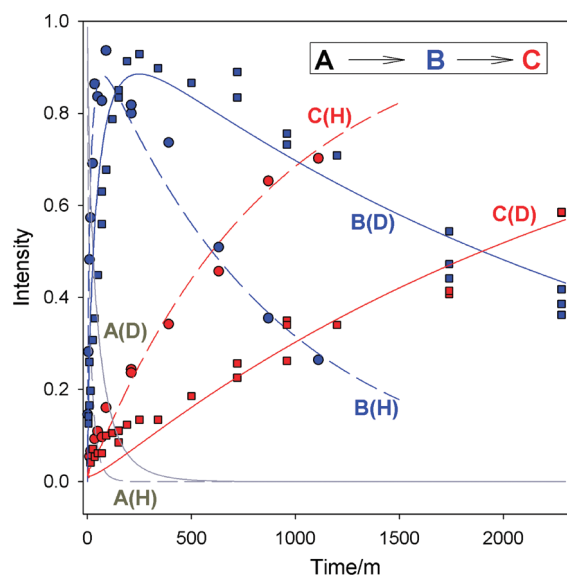


**FIGURE 8.** Step-annealing curves (253 K) of hydride intermediate (**A**), leading to formation of **B** intermediate and ground state **C**, in  $H_2O/D_2O$  buffers. Fits to distributed (stretched exponential) two-step relaxation:  $t_1(H_2O) = 13$  min,  $t_1(D_2O) = 49$  min;  $t_2(H_2O) = 870$  min,  $t_2(D_2O) = 2700$  min. For clarity, data for **A(H)** and **A(D)** are omitted, and only the fits are presented.

With this protocol, we showed that the hydride intermediate (**A**) relaxes to the resting state (**C**) in two steps,  $A \rightarrow B \rightarrow C$ . Both steps show appreciable solvent kinetic isotope effects,  $KIE \approx 3-4$  (85%  $D_2O$ ) (Figure 8), assigned to the generation of  $H_2$  during relaxation. According to the LT scheme, Figure 1, this intermediate must then be the catalytically central  $E_4$  state that has been activated for  $N_2$  binding and reduction by the accumulation of four electrons. Its relaxation by loss of  $H_2$  generates the state **B** =  $E_2$ , and this relaxes with loss of  $H_2$  to the resting state, **C** =  $E_0$ .

We propose that the combination of this relaxation protocol with ENDOR/ESEEM studies of structure offers a real prospect of connecting trapped  $E_n$  intermediates to mechanism. Beyond that, it will help to characterize individual intermediates and enable us to distinguish among the multiplicity of reaction pathways that are revealed when considering alternate “inventory routes”, as in Figure 7. For example, if the same intermediate is trapped during turnover with diazene and hydrazine, then the two should show the same relaxation behavior.

## The Many Faces of Nitrogenase

This Account has discussed progress and prospects for determination of an “ $N_2$  reduction mechanism” defined as comprising the reaction pathway detailing the composition and structure of intermediates, the substrate reduction “route” that links those intermediates to kinetics through the

determination of  $n$ , and the electron inventory for each. As noted above, the perspectives of Schrock<sup>7</sup> and of Howard and Rees<sup>6</sup> provide a context for this work and discuss challenges not addressed in this Account, the other unclimbed “faces of the nitrogenase mountain”. Three issues noted here are of particular relevance to the efforts described here: (i) Do the bound intermediates “migrate” over FeMo-co during catalysis and is Mo directly involved at some stage?<sup>7,9</sup> (ii) What is **X** (Figure 1)?<sup>17</sup> (iii) How does the P cluster participate?<sup>42</sup> The first two of these can be addressed by ENDOR studies of trapped intermediates, the third by relaxation measurements. But such challenges will require much “climbing” by us and others before they can be discussed in some future Account.

## The Climb

At the start of this millennium, the “face” of nitrogenase discussed here was shrouded in clouds. This discussion has argued that strategies have been formulated that bring this face into view and afford approaches to its climb. This does not mean that this summit will soon be reached but rather that vigorous climbing will be rewarded.

*B.M.H. thanks Prof. R. H. Holm for insights into the mysteries of “mechanism”. This work has been supported by the National Institutes of Health (Grants HL13531 [B.M.H.], GM59087 [L.S. and D.R.D.]) and the National Science Foundation (Grants MCB 0723330 [B.M.H.]) and MCB 071770 [D.R.D.].*

## BIOGRAPHICAL INFORMATION

**Brian M. Hoffman** was an undergraduate at the University of Chicago, received his Ph.D. from Caltech (Harden McConnell), and spent a postdoctoral year at MIT (Alex Rich). From there, he went to Northwestern University, where he is the Charles E. and Emma H. Morrison Professor in the Departments of Chemistry and of Biochemistry Molecular Biology & Cell Biology.

**Dennis R. Dean** received a B.A. from Wabash College and a Ph.D. from Purdue University (Arthur Aronson) and was a postdoctoral at the University of Wisconsin (Masayasu Nomura). Currently he is the Stroobants Professor of Biotechnology at Virginia Tech, where he also serves as the Director of the Fralin Life Science Institute and Associate Director of the VT-Carilion Medical Research Institute.

**Lance C. Seefeldt** received a B.S. degree from the University of Redlands and a Ph.D. from the University of California at Riverside (Dan Arp). He was a postdoctoral fellow in the Center for Metalloenzyme Studies at the University of Georgia (Len Mortenson) and is now Professor of Chemistry and Biochemistry at Utah State University.

## FOOTNOTES

\*Corresponding author. E-mail: bmh@northwestern.edu.

<sup>†</sup>E-mail addresses: deandr@vt.edu; lance.seefeldt@usu.edu.

## REFERENCES

- Zhao, Y.; Bian, S.-M.; Zhou, H.-N.; Huang, J.-F. Diversity of nitrogenase systems in diazotrophs. *J. Integr. Plant Biol.* **2006**, *48*, 745–755.
- Burgess, B. K.; Lowe, D. L. Mechanism of molybdenum nitrogenase. *Chem. Rev.* **1996**, *96*, 2983–3011.
- Thorneley, R. N. F.; Lowe, D. J. In *Molybdenum Enzymes*; Spiro, T. G., Ed.; Wiley-Interscience: New York, 1985; Vol. 7; pp 89–116.
- Wilson, P. E.; Nyborg, A. C.; Watt, G. D. Duplication and extension of the Thorneley and Lowe kinetic model for *Klebsiella pneumoniae* nitrogenase catalysis using a MATHEMATICA software platform. *Biophys. Chem.* **2001**, *91*, 281–304.
- Rees, D. C.; Tezcan, F. A.; Haynes, C. A.; Walton, M. Y.; Andrade, S.; Einsle, O.; Howard, J. B. Structural basis of biological nitrogen fixation. *Philos. Trans. R. Soc., A* **2005**, *363*, 971–984.
- Howard, J. B.; Rees, D. C. How many metals does it take to fix N<sub>2</sub>? A mechanistic overview of biological nitrogen fixation. *Proc. Natl. Acad. Sci. U.S.A.* **2006**, *103*, 17088–17093.
- Schrock, R. R. Reduction of dinitrogen. *Proc. Natl. Acad. Sci. U.S.A.* **2006**, *103*, 17087.
- Seefeldt, L. C.; Dean, D. R.; Hoffman, B. M.; Dos Santos, P. C.; Barney, B. M.; Lee, H.-I. Breaking the N<sub>2</sub> triple bond: insights into the nitrogenase mechanism. *Dalton Trans.* **2006**, 2277–2284.
- Dos Santos, P. C.; Igarashi, R. Y.; Lee, H.-I.; Hoffman, B. M.; Seefeldt, L. C.; Dean, D. R. Substrate interactions with the nitrogenase active site. *Acc. Chem. Res.* **2005**, *38*, 208–214.
- Seefeldt, L. C.; Hoffman, B. M.; Dean, D. R. Mechanism of Mo-dependent nitrogenase. *Annu. Rev. Biochem.* **2009**, in press.
- Davis, L. C.; Henzl, M. T.; Burris, R. H.; Orme-Johnson, W. H. Iron-sulfur clusters in the molybdenum-iron protein component of nitrogenase. Electron paramagnetic resonance of the carbon monoxide inhibited state. *Biochemistry* **1979**, *18*, 4860–4869.
- Cameron, L. M.; Hales, B. J. Investigation of CO binding and release from Mo-nitrogenase during catalytic turnover. *Biochemistry* **1998**, *37*, 9449–9456.
- Einsle, O.; Tezcan, F. A.; Andrade, S. L. A.; Schmid, B.; Yoshida, M.; Howard, J. B.; Rees, D. C. Nitrogenase MoFe-protein at 1.16 Å resolution: A central ligand in the FeMo-cofactor. *Science* **2002**, *297*, 1696–1700.
- Schrock, R. R. Catalytic reduction of dinitrogen to ammonia at a single molybdenum center. *Acc. Chem. Res.* **2005**, *38*, 955–962.
- Eady, R. R. Structure–function relationships of alternative nitrogenases. *Chem. Rev.* **1996**, *96*, 3013–3030.
- Madden, M. S.; Paustian, T. D.; Ludden, P. W.; Shah, V. K. Effects of homocitrate, homocitrate lactone, and fluorohomocitrate on nitrogenase in NifV- mutants of *Azotobacter vinelandii*. *J. Bacteriol.* **1991**, *173*, 5403–5405.
- Lukoyanov, D.; Pelmenshikov, V.; Maeser, N.; Laryukhin, M.; Yang, T. C.; Noodleman, L.; Dean, D.; Case, D.; Seefeldt, L.; Hoffman, B. Testing if the interstitial atom, X, of the nitrogenase molybdenum-iron cofactor is N or C: ENDOR, ESEEM, and DFT studies of the S = 3/2 resting state in multiple environments. *Inorg. Chem.* **2007**, *46*, 11437–11449.
- Blankenship, R. E. *Molecular Mechanisms of Photosynthesis*, 1st ed.; Blackwell Science, Ltd.: Oxford, U.K., 2002.
- Sorlie, M.; Christiansen, J.; Lemon, B. J.; Peters, J. W.; Dean, D. R.; Hales, B. J. Mechanistic features and structure of the nitrogenase  $\alpha$ -Gln195 MoFe protein. *Biochemistry* **2001**, *40*, 1540–1549.
- Fisher, K.; Dilworth, M. J.; Newton, W. E. Differential effects on N<sub>2</sub> binding and reduction, HD formation, and azide reduction with  $\alpha$ -195His- and  $\alpha$ -191Gln-substituted MoFe proteins of *Azotobacter vinelandii* nitrogenase. *Biochemistry* **2000**, *39*, 15570–15577.
- Lee, H.-I.; Igarashi, R. Y.; Laryukhin, M.; Doan, P. E.; Dos Santos, P. C.; Dean, D. R.; Seefeldt, L. C.; Hoffman, B. M. An organometallic intermediate during alkyne reduction by nitrogenase. *J. Am. Chem. Soc.* **2004**, *126*, 9563–9569.
- Lee, H.-I.; Sørlie, M.; Christiansen, J.; Yang, T.-C.; Shao, J.; Dean, D. R.; Hales, B. J.; Hoffman, B. M. Electron inventory, kinetic assignment (E<sub>n</sub>), structure, and bonding of nitrogenase turnover intermediates with C<sub>2</sub>H<sub>2</sub> and CO. *J. Am. Chem. Soc.* **2005**, *127*, 15880–15890.
- Igarashi, R. Y.; Laryukhin, M.; Santos, P. C. D.; Lee, H.-I.; Dean, D. R.; Seefeldt, L. C.; Hoffman, B. M. Trapping H<sup>+</sup> bound to the nitrogenase FeMo-cofactor active site during H<sub>2</sub> evolution: Characterization by ENDOR spectroscopy. *J. Am. Chem. Soc.* **2005**, *127*, 6231–6241.

- 24 Barney, B. M.; Laryukhin, M.; Igarashi, R. Y.; Lee, H.-I.; Santos, P. C. D.; Yang, T.-C.; Hoffman, B. M.; Dean, D. R.; Seefeldt, L. C. Trapping a hydrazine reduction intermediate on the nitrogenase active site. *Biochemistry* **2005**, *44*, 8030–8037.
- 25 Barney, B. M.; Yang, T.-C.; Igarashi, R. Y.; Santos, P. C. D.; Laryukhin, M.; Lee, H.-I.; Hoffman, B. M.; Dean, D. R.; Seefeldt, L. C. Intermediates trapped during nitrogenase reduction of  $\text{N}\equiv\text{N}$ ,  $\text{CH}_3\text{-N}=\text{NH}$ , and  $\text{H}_2\text{N-NH}_2$ . *J. Am. Chem. Soc.* **2005**, *127*, 14960–14961.
- 26 Barney, B. M.; Lukoyanov, D.; Yang, T.-C.; Dean, D. R.; Hoffman, B. M.; Seefeldt, L. C. A methylidiazene ( $\text{HN}=\text{N-CH}_3$ )-derived species bound to the nitrogenase active-site FeMo cofactor: Implications for mechanism. *Proc. Natl. Acad. Sci. U.S.A.* **2006**, *103*, 17113–17118.
- 27 Barney, B. M.; McCleod, J.; Lukoyanov, D.; Laryukhin, M.; Yang, T. C.; Hoffman, B. M.; Dean, D. R.; Seefeldt, L. C. Diazene ( $\text{HN}=\text{NH}$ ) is a substrate for nitrogenase: Insights into the pathway of  $\text{N}_2$  reduction. *Biochemistry* **2007**, *46*, 6784–6794.
- 28 Hoffman, B. M.; DeRose, V. J.; Doan, P. E.; Gurbel, R. J.; Houseman, A. L. P.; Telsler, J. Metalloenzyme active-site structure and function through multifrequency CW and pulsed ENDOR. *Biol. Magn. Reson* **1993**, *13* (EMR of Paramagnetic Molecules), 151–218.
- 29 Schweiger, A.; Jeschke, G. *Principles of Pulse Electron Paramagnetic Resonance*; Oxford University Press: Oxford, U.K., 2001.
- 30 Christie, P. D.; Lee, H.-I.; Cameron, L. M.; Hales, B. J.; Orme-Johnson, W. H.; Hoffman, B. M. Identification of the CO-binding cluster in nitrogenase MoFe protein by ENDOR of  $^{57}\text{Fe}$  isotopomers. *J. Am. Chem. Soc.* **1996**, *118*, 8707–8709.
- 31 Lee, H.-I.; Cameron, L. M.; Hales, B. J.; Hoffman, B. M. CO binding to the FeMo cofactor of CO-inhibited nitrogenase:  $^{13}\text{C}$ O and  $^1\text{H}$  Q-band ENDOR investigation. *J. Am. Chem. Soc.* **1997**, *119*, 10121–10126.
- 32 Pickett, C. J. The Chatt cycle and the mechanism of enzymic reduction of molecular nitrogen. *JBIC, J. Biol. Inorg. Chem* **1996**, *1*, 601–606.
- 33 Hinnemann, B.; Norskov, J. K. Chemical activity of the nitrogenase FeMo cofactor with a central nitrogen ligand: Density functional study. *J. Am. Chem. Soc.* **2004**, *126*, 3920–3927.
- 34 Dilworth, M. J.; Thorneley, R. N. F. Nitrogenase of *Klebsiella pneumoniae*. Hydrazine is a product of azide reduction. *Biochem. J.* **1981**, *193*, 971–983.
- 35 Davis, L. C. Hydrazine as a substrate and inhibitor of *Azotobacter vinelandii* nitrogenase. *Arch. Biochem. Biophys.* **1980**, *204*, 270–276.
- 36 Lees, N. S.; McNaughton, R. L.; Gregory, W. V.; Vela, J.; Holland, P. L.; Hoffman, B. M. ENDOR characterization of a synthetic diiron hydrazido complex as a model for nitrogenase intermediates. *J. Am. Chem. Soc.* **2008**, *130*, 546–555.
- 37 Mehn, M. P.; Peters, J. C. Mid- to high-valent imido and nitrido complexes of iron. *J. Inorg. Biochem.* **2006**, *100*, 634–643.
- 38 Holland, P. L. Electronic structure and reactivity of three-coordinate iron complexes. *Acc. Chem. Res.* **2008**, *41*, 905–914.
- 39 Lukoyanov, D.; Barney, B. M.; Dean, D. R.; Seefeldt, L. C.; Hoffman, B. M. Connecting nitrogenase intermediates with the kinetic scheme for  $\text{N}_2$  reduction by a relaxation protocol and identification of the  $\text{N}_2$  binding state. *Proc. Natl. Acad. Sci. U.S.A.* **2007**, *104*, 1451–1455.
- 40 Lowe, D. J.; Fisher, K.; Thorneley, R. N. F. *Klebsiella pneumoniae* nitrogenase. Mechanism of acetylene reduction and its inhibition by carbon monoxide. *Biochem. J.* **1990**, *272*, 621–5.
- 41 Davydov, R.; Matsui, T.; Fujii, H.; Ikeda-Saito, M.; Hoffman, B. M. Kinetic isotope effects on the rate-limiting step of heme oxygenase catalysis indicate concerted proton transfer/heme hydroxylation. *J. Am. Chem. Soc.* **2003**, *125*, 16208–16209.
- 42 Chan, J. M.; Christiansen, J.; Dean, D. R.; Seefeldt, L. C. Spectroscopic evidence for changes in the redox state of the nitrogenase P-cluster during turnover. *Biochemistry* **1999**, *38*, 5779–5785.